FATIGUE IN RATE DEPENDENT ALLOY

Y. Katz and A. Bussiba *

Fatigue crack propagation stage was investigated in Zn-22Al eutectoid superplastic alloy. Basic mechanical properties were established and tension-tension fatigue tests were performed following fracture mechanics methods. Fatigue crack extension rate curves at 296K and 375K were determined utilizing notched specimens. Tests were carried out under stress-intensity amplitude controlled conditions, in a frequency range between 0.1 up to 80 Hz. In addition, monotonic tests were performed in order to elaborate on thermal effects and the strain-rate sensitivity. Experimental results and fractographic observations are described and analysed in terms of generalized view on fatigue processes in time sensitive materials.

INTRODUCTION

Linear elastic fracture mechanics is limited to account for relatively large scale plasticity effects in general, and during fatigue processes in particular. This limitation is more evident in the case of some rate sensitive materials, since, additional factors influence the local mechanical environment at or near the fatigue crack front. Generally, such behaviour might be also typical to plastic processes at relatively high temperatures, where a significant contribution of the time dependent factor is inevitable.

At least two influencial origins are realized in fatigue processes in time-sensitive material. First, the contribution of the time dependent term, in the sense of a creep component. Secondly , the contribution of the pure fatigue component, including thermal influences and frequency effects on the yield stress, plastic flow behaviour, plastic zone characterization, relaxation effects, typical fracture modes and mode transitions.

Both authors are with the Nuclear Research Centre-Negev
P.O.B. 9001 Beer-Sheva 84190, ISRAEL.

Despite the mentioned restrictions, the current study is centered on the Zn-22Al superplastic alloy tested at selective temperature and frequency range, where fracture mechanics concepts still prevail. Although the present selected alloy is superplastic at 495K, significant rate sensitivity is obtained even at ambient temperatures caused by the kind of residual superplasticity state. Considering this range, quite remarkable effects are expected in the present crystalline material, without the need to apply relatively high temperatures and a wide range of strain-rate or frequency experimentation.

In contrast to the considerable attention which has been directed at elucidating the superplastic deformation mechanisms (including the typical behaviour of the Zn-22Al alloy), very little research activity has been invested in the cyclic behaviour of superplastic systems. The present paper is concerned with fatigue processes in such an alloy with two fold primary objectives. Firstly, to investigate the typical cyclic behaviour of a superplastic alloy. Secondly, to examine and extend this study on fatigue damage according to fundamental concepts. In fact establishing a more global view on fatigue crack nucleation and propagation in visco-elastic-plastic materials, is intended.

Langdon (1) has investigated the fracture process in superplastic flow. Even in the monotonic case, the fracture stage appeared quite complex. In fact superplasticity can be developed only by the supression of competitive events in order to use the capability of very high uniaxial elongations. Accordingly, Langdon has emphasized two basic requirements for optimum conditions of superplastic flow. (i) a supression of localized (but not diffuse) necking, and (ii) a supression of significant cavity interlinkage (but not necessarily of cavity nucleation and growth). As mentioned the current study adopts fracture mechanics methods with emphasis on the crack extension stage, incorporating complementary aspects as arise from metallographic and fractographic observations.

Experimental Procedure

Experiments were conducted on the superplastic Zn-22Al eutectoid alloy that was received in the form of sheet of 8.5 mm in thickness. Composition analysis and microstructural characterization were performd by X-ray diffraction and metallographic observations. Uniaxial tensile tests were carried out in order to determine the basic mechanical properties up to 470K at various strain rate conditions between 10^{-5} up to 10^{1} sec^{-1}. Prior to the fatigue testing monotonic fracture resistance properties were searched for, particulary at ambient temperatures. For the monotonic and cyclic fracture mechanics studies, compact pre-fatigued single edge notched specimens were utilized. Tension-tension fatigue was applied (for $R \simeq 0$ in order to minimize load interactive effects) controlled by the stress intensity range (ΔK) amplitudes. At room tempera-

ture the frequency varied between 0.1 to 80 Hz, while at 375K selective tests were performed at 20 and 80 Hz. Generally, a closed loop electrohydraulic machine was used with temperature control and appropriate instrumentation for crack length or crack opening displacement(COD) measurments. Additionally, fracture mechanics parameters were established including rate sensitivity with some reference to the low temperature behaviour at 77K,where negligible residual viscous contribution is really expected.

Actually, the present mechanical scheme provided information regarding the monotonic and cyclic behavior in terms of stress-strain curves, plastic stress vs. strain rate ($\dot{\varepsilon}$), strain rate sensitivity coefficient (m), and fatigue crack extension rate curves (da/dN vs. ΔK).

In addition, light and electron metallography and fractography investigation was performed. In fact the fatigue crack growth was tracked along the different crack extension stages from the near threshold (ΔK_{th}) up to the fatigue critical values (ΔK_{fc}). Metallurgical parameters, monotonic and cyclic fracture modes, as well as secondary cracking study were included in the present experimental program.

Experimental Results

The microstructure consisted of the Al-rich and the Zn-rich phases with very fine equiaxed grains about 1.4μm in size (Figs.1 and 2). This microduplex structure was confirmed also by X-ray diffraction technique.
Fig.3 shows the uniaxial plastic deformation stage obtained from an interrupted test at 420K and strain rate of $1x10^{-3}$ sec^{-1}. The typical true stress-strain curve for 296K is shown in Fig.4, while some of the basic mechanical properties are summarized in Table 1.

Fig.5 illustrates the unique deformation capacity obtained during uniaxial tensile tests at various temperatures. As indicated, a significant degree of high plasticity occurred even at ambient temperatuers. Fig.6 demonstrates the strain-rate sensitivity coefficient m vs.$\dot{\varepsilon}$ at different temperatures. Notice the increase of m at 470K up to 0.7 as compared to about 0.4 at 296K. Generally, the optimal conditions associated with the maximum value of m are shifted to the right with the temperature i.e. higher values of $\dot{\varepsilon}$ are needed at higher temperatures. For example, thermal variation between 296K to 470K resulted in $\dot{\varepsilon}$ shifting from about 10^{-3}up to $5X10^{-2}sec^{-1}$. Fig.7 demonstrates the true plastic stress dependency on $\dot{\varepsilon}$at various testing temperatures.

Fatigue crack extension rate curves da/dN vs.ΔK are illustrated in Figs.8 (a) and 8 (b) for 296K and 375K respectively. The frequency effect is noted as well, with a significant increase of the rate at higher temperatures. Here too, the influencial effects of f

are readily observed even at ambient temperatures. In Fig.9 the dependency of the crack growth rate on the frequency is shown along the different fatigue stages in a more illustrative fashion.

TABLE 1 - Basic Mechanical Properties for the Zn-22Al at Various Temperatures and Strain Rates.

Temp. K	Yield Stress 0.2 offset $\sigma_{0.2}$ MPa		Ultimate Tensile Stress σ_u MPa		Critical Stress Intensity Factor K_c MPa·m$^{1/2}$
$\dot{\varepsilon}$(sec^{-1})	5.3×10^{-3}	5.3×10^{0}	5.3×10^{-3}	5.3×10^{0}	
77	310	365	420	440	7.5
296	170	270	225	330	28.0
350	85	240	100	310	-
420	25	135	31	200	-
470	5	120	7	150	-

* Determined for a cross head speed of 1 mm/sec.

Fig.10 (a) indicates a typical subcritical fatigue crack at 296K, with emphasis on its sharpness, growing under cyclic loading at 50 Hz.

In fact, high temperature or low frequency caused drastic changes of the crack tip, mainly reflected in blunting which occurred, as illustrated in Fig.10 (b). Figs.11 (a) and 11 (b) show fractographic findings with emphasis on the fatigue fracture mode variations affected by rate and thermal influences. The role of grain boundaries in the crack propagation processes is particularly stressed and is clearly observed.

Discussion

Fatigue processes in rate sensitive solids have been studied theoretically by Wnuk (2) and are viewed as a sequence of slow growth periods, described by a non-linear differential equation of the first order. In this theoretical study the total rate of crack growth is expressed by two terms; the familiar power law for high cycle range and limited plasticity, while the second accounts for the time-dependent contribution.

Low cycle fatigue of superplastic aluminium bronze has been addressed by Gandhi et al (3) over the temperature range from ambient to 1073K. The fatigue testing has been controlled by the plastic strain amplitudes and the results actually fit the Manson-Coffin law with certain deviations from the usual fatigue nature of non-superplastic metallic systems.

Woodthorpe and Pearce (4) have investigated the frequency effect in fatigue of Zn-22Al alloy. The fatigue tests have been performed over the frequency range 8-100 Hz and over a temperature range 293-393K. Life variation with the frequency, has been expressed by S-N curves indicating a marked frequency effect even at ambient temperatures. Higher frequency resulted in a significant increase of the total cycles to failure.

Considering the subcritical fatigue crack in the range $\Delta K_{th} < \Delta K < \Delta K_{fc}$, the present experimental study confirms the typical sigmoidal function for the fatigue crack propagation rate in the Zn-22Al alloy. Moreover, the frequency affects strongly the FCPR with similar tendencies as concluded from the already mentioned low cycle fatigue investigation (4). There, distinction has been made between two stages of crack growth, attributing the frequency effects to the initial crack growth stage where the cumulative damage is more expressed by slip processes. Such a degree of frequency sensitivity is more typical to visco-elastic-plastic polymeric systems. Bussiba et al (5) have investigated the frequency effects in PMMA and polycarbonat exposed to cyclic loading, recognizing other related aspects that introduce additional competitive factor in plastics. For example, high thermal sensitivity is more pronounced in high frequency testing and might enhance the FCPR and partially mask the intrinsic effects caused by the frequency as a kind of isolated and independent parameter.

The present study followed fracture mechanics methods and the fatigue curves in stage II could be expressed empirically by a power law dependency, as proposed for example by Paris and Erdogen (6). For the sake of briefness only one argument is presented explaining the frequency behaviour as determined experimentally. Generally, power law dependency in fatigue is obtained by following various patterns of analysis. For example, Weertman (7) has used the Bilby et al (8) dislocation model of fatigue crack growth by imposing the criterion that fracture occurs at the pre-existing crack tip whenever the cumulative plastic displacement achieves a critical value which is a characteristic of the material. The localized fracture criterion is clearly related to the fundamental plastic flow behaviour according to the general concepts regarding an appropriate criterion for time dependent crack growth. Attempts concerning these issues have been addressed by Williams (9) and by Christensen (10).

Nevertheless, rapid processes probably obey a nearly elastic dependency between the stress and the strain. In contrast, long-time processes need a rate dependent generalization for fracture criterion. In the current investigation an additional complexity occurs caused by variations of the crack tip due to crack blunting processes affecting the localized stress field. Accordingly, the experimental results indicate significant rate effects, which are probably reduced due to the competitive processes (in the sense of crack tip blunting) resulting in a certain moderation of the rate dependent term . This damage contribution is expected in long-time processes, in addition to the pure cyclic extension with no interactive effects.

Empirically, the fatigue crack growth rate variation with f can be described by the same type of relationship which has been proposed by Yokobori et al (11), based on the dislocation dynamic theory for fatigue crack propagation. However, through completely different reasoning, the inverse dependency of the crack extension rate with f has also been proposed by Yokobori et al (12) in the case of fatigue and creep interaction, namely, the crack extension rate is given by:

$$da/dN = A\ \Delta K^{n}\ f^{-\alpha} \quad \ldots\ldots\ldots\ldots\ldots\ldots (1)$$

For the Zn-22Al alloy α values up to about 0.3 (for stage II extension) were determined in the current study at 296K. James (13) has suggested the same equation which has been applied by Plumtree and Yu (14) for AISI 304 stainless steel, tested under cyclic loading at 843K. In this case α=0.12 has been determined. Similar approach has been expressed by Guinemer and Plumtree (15) and Solomon and Coffin (16) while attributing the frequency effect to a creep component or creep fatigue interaction. Higher values for α have been obtained in PVC system of about 0.37 - 0.8 (17) and 0.4 for polystyrene at amplitude range of ΔK= 0.55 MPa$\cdot m^{1/2}$ (18).

The geometrical factor in terms of crack tip blunting was influenced in the Zn-22Al alloy by temperature and f. High temperature or low f, resulted in crack tip blunting as shown in Fig.10 (b). The fatigue fracture mode was dominated by the intergranular crack extension mode which masked the typical continuum fracture mode in the sense of fatigue striations. At higher temperatures secondary intergranular microcracking coalescence occurred as shown in Fig.11 (b). Basically, no mode transition occurred above the ductile-brittle transition temperature. At low temperatures completely different mechanism really dominated, as reflected also by the fatigue crack extension curve as described by Katz et al (19) elsewhere.

In conclusion, fatigue crack extension in superplastic Zn-22Al is highly sensitive to the cyclic frequency even at ambient temperatures. Consequently, the selected material can serve as modelling

material in studying (at ambient temperatures) fatigue in rate dependent metallic systems. As found, fatigue crack propagation is dominated by intergranular fracture mode, which is also the characteristic fracture mode in monotonic loading, even at the optimal superplastic conditions.

SYMBOLS USED

A = constant in Paris law equation

da/dN = fatigue crack extension rate (mm/cycle)

e = elongation (%)

f = frequency (Hz)

FCPR = fatigue crack propagation rate

Kc = critical stress intensity factor ($MPa.m^{1/2}$)

m = strain rate sensitivity coefficient

n = numerical exponent

R = load ratio

α = numerical exponent

$\dot{\varepsilon}$ = true strain rate (sec^{-1})

σ = stress (MPa)

ΔK_{fc} = fatigue critical stress intensity range ($MPa\ m^{1/2}$)

ΔK = Cyclic stress intensity range ($MPa \cdot m^{1/2}$)

ΔK_{th} = threshold stress intensity range ($MPa \cdot m^{1/2}$)

REFERENCES

1. Langdon, T.G., Metal Science, Vol. 16, 1982, pp.175-183.
2. Wnuk. M. P., Int. J. of Fracture, Vol.10, 1974, pp.223-226.
3. Gandhi. C., Rama Rao, P. and Taplin, D.M. R., Metal Science, Vol.12, 1978, pp.30-34.
4. Woodthorpe, J. and Pearce, R., Metal Science, Vol.11, 1977, pp.103-108.
5. Bussiba, A., Katz, Y. and Mathias, H. "Fatigue crack propagation in polymers", Second Israel Material Engineering Conference Proceedings, Beer-Sheva, Israel, Edited by A. Grill and S.I. Rokhlin. 1984.
6. Paris, P. and Erdogen, F., Trans. ASME J. Basic Eng., V. 85., 1963 p.528.
7. Weertman, J., Int. J. Fract., Mech. Vol.2, 1966, p.460.

8. Bilby, B. A., Cottrell, A. H. and Swinden, K. H., Proc. Roy. Soc., A272, 1963, p.304.

9. Williams, M, L., Int. J. of Fract. Mech., Vol.1, 1965, p.297

10. Christensen, R. M., Int. J. of Fract. Vol.15. 1979, pp.3-21.

11. Yokobori, T. and Sato, K., Eng. Fract. Mech., Vol.8, 1976, pp.81-88.

12. Yokobori, T., Ichikawa, M. and Yokobori Jr. A. T., Eng. Fract. Mech., Vol.7, 1975 pp.441-443.

13. James, L. A., "Frequency Effects in the Elevated Temperature Crack Growth Behaviour of Austenitic Steel", Proc. Pressure Vessel and Piping Conf., CSME/ASME Montreal, Canada, June 1978.

14. Plumtree, A. and Yu, M.,"Thermal and Environmental Effects in Fatigue: Research - Design Interface", Eds. C. E. Jaske, S. Y. Hudak Jr. and M. E. Mayfield, ASME, 1983, pp.13-19.

15. Guinemer, J. Y. and Plumtree, A., "An Elevated Temperature Fatigue Crack Model for Stainless Steels", Mechanical Testing for Deformation Model Development, Edited by Rohde, R. W. and Swearengen, J. C., STP 676, ASTM, Philadelphia, U.S.A., 1982 pp.452-456.

16. Solomon, H. D. and Coffin Jr. L. F., "Effects of Frequency and Environment on Fatigue Crack Growth in A286 at 1100F ", Fatigue at Elevated Temperatures, Edited by Carden, A. E., et al, STP 520, ASTM, Philadelphia, U.S.A., 1973 pp.112-121.

17. Radon, J. C., Int. J. of Fract., Vol.16, 1980, pp.533-552.

18. Skibo, M. D., Hertzberg, R. W. and Manson, J. A. "The Effect of Temperature on the Frequency Sensitivity of Fatigue Crack Propagation in Polymers", Proceedings of the ICF4. Vol.3, Edited by D.M.R. Taplin, University of Waterloo Press, Waterloo Ontario, Canada, 1977, pp.1127-1133.

19. Katz, Y., Bussiba, A. and Mathias, H., Advences in Cryogenic Materials, Vol.30, 1984, pp.339-347.

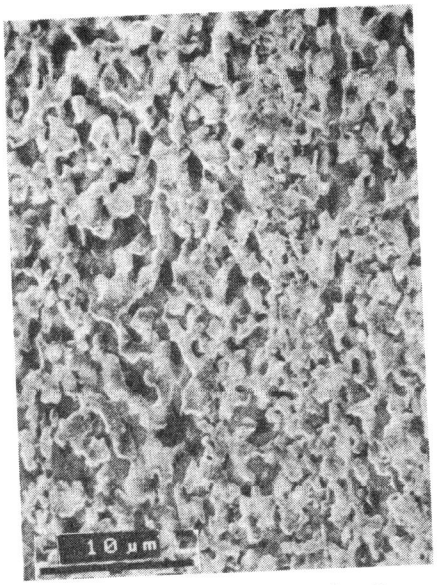

Figure 1. SEM metallography-Zn-22Al microstructure

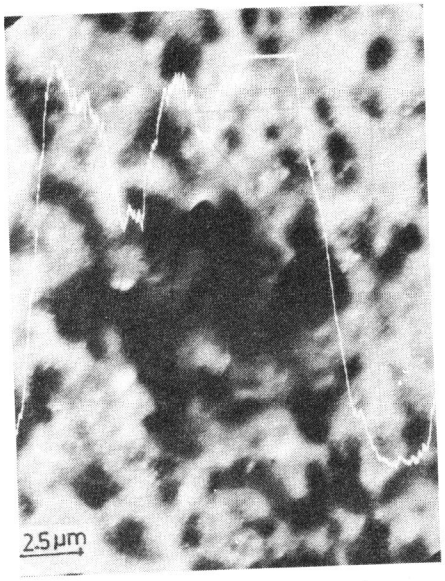

Figure 2. Microduplex structure-line scan profile in Al rich phase

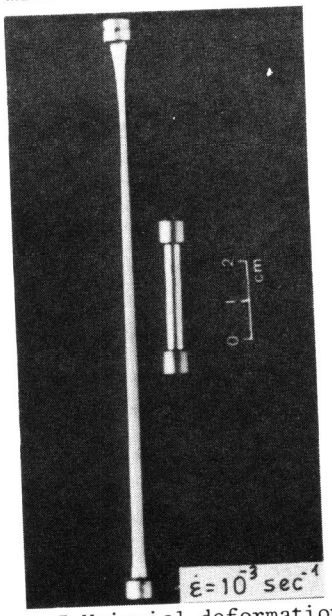

Figure 3. Uniaxial deformation stage at 420K for $\dot{\varepsilon}=1.10^{-3}$ Sec-1

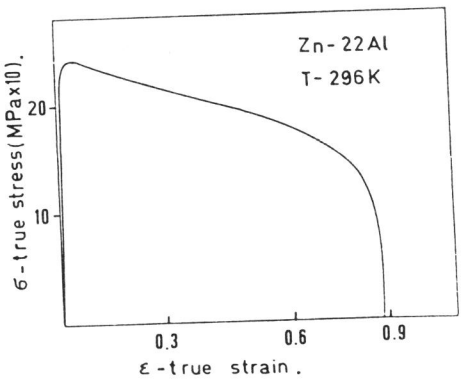

Figure 4. True tensile stress-strain curve at 296K

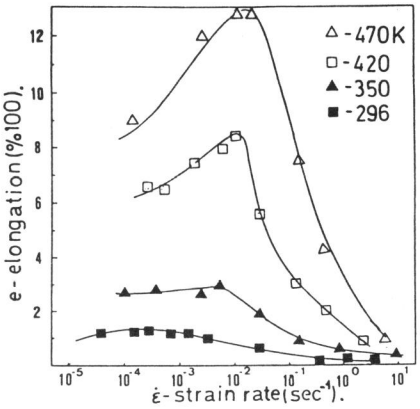

Figure 5. Tensile elongation vs. $\dot{\varepsilon}$ at various temperatures

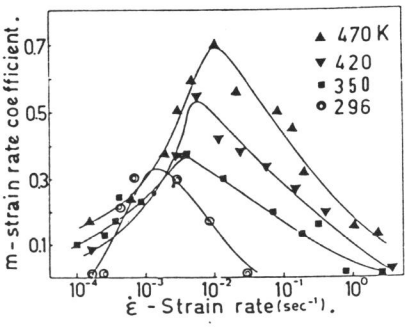

Figure 6. m vs. $\dot{\varepsilon}$ at various temperatures

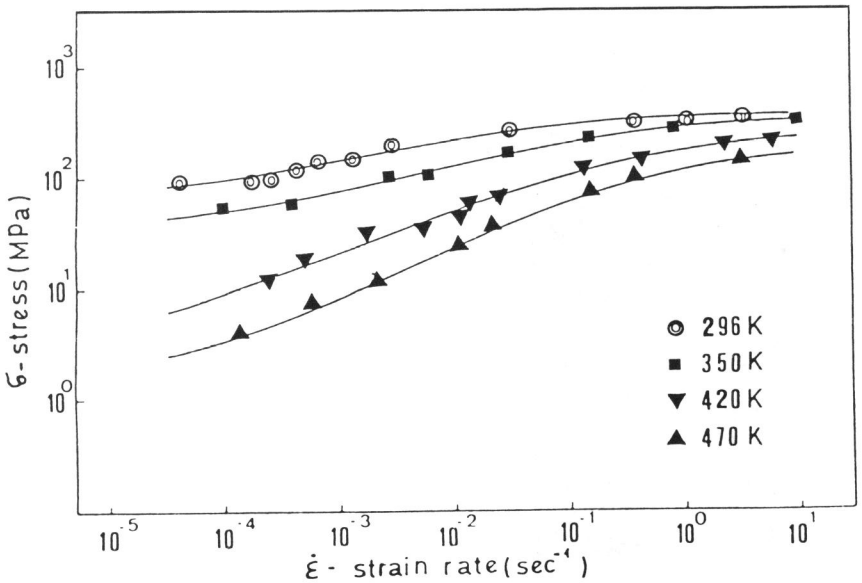

Figure 7. Tensile plastic stress vs. $\dot{\varepsilon}$ at various temperatures

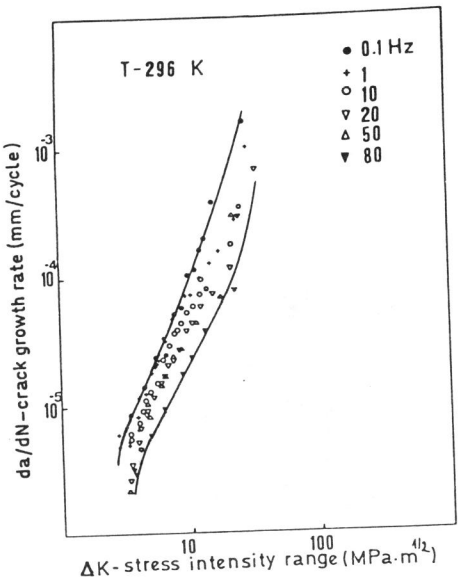

Figure 8(a). FCPR vs. ΔK at 296K, for frequency 0.1-80Hz

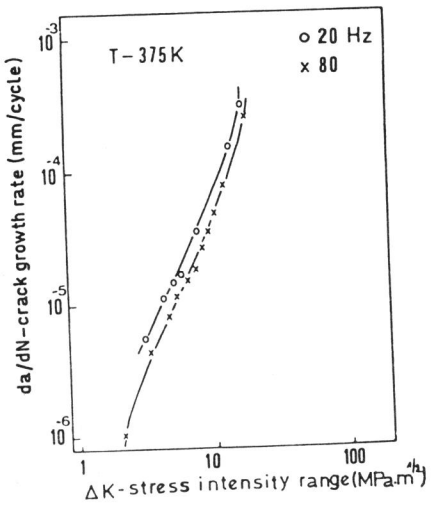

Figure 8(b). FCPR vs. ΔK at 375K, for frequencies, 20Hz, 80Hz

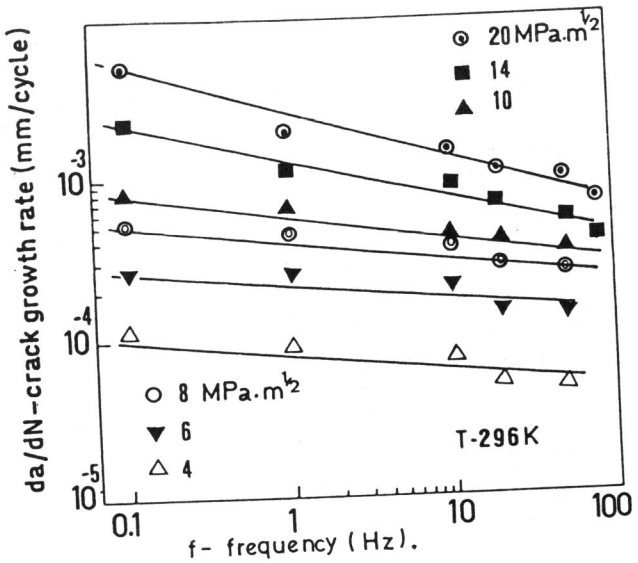

Figure 9. FCPR vs. f at 296K for various ΔK

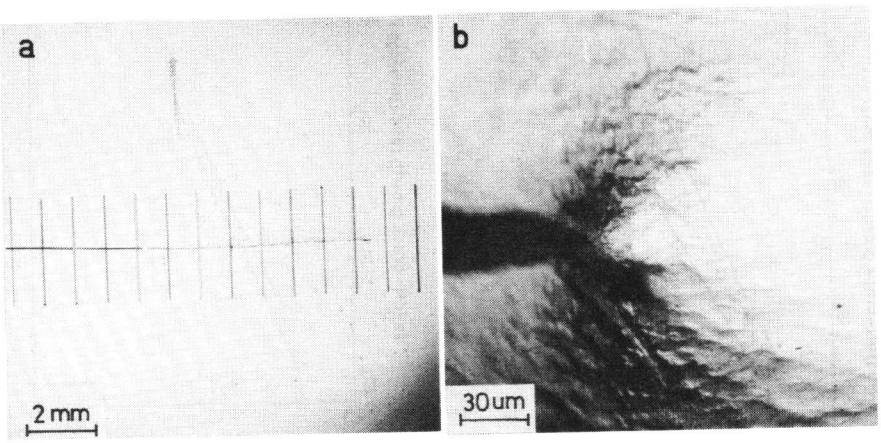

Figure 10. Fatigue crack extension tip (a) sharp tip at 296K for 50 Hz (b) blunted tip at 400K for f = 10Hz

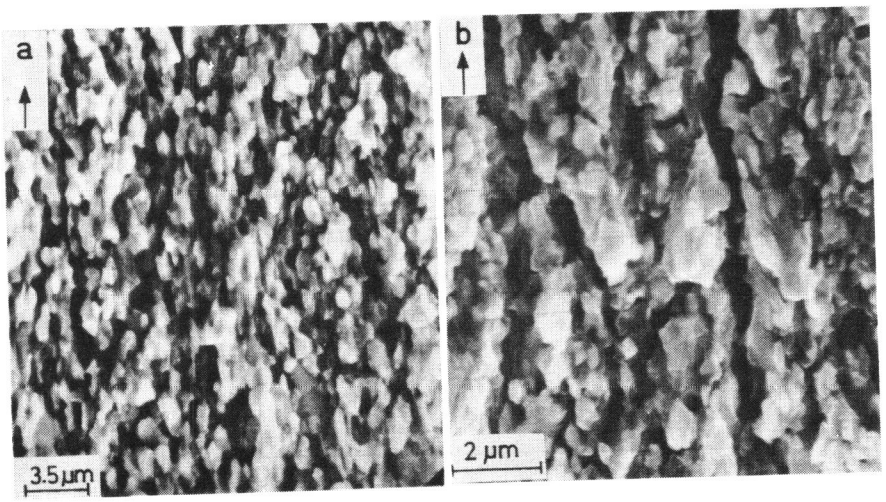

Figure 11. SEM fractography (a) intergranular mode at 296K (b) intergranular cracking coalescence at 420K